Rarefied Gas Dynamics, Vol. 1, Academic Press, New York, 1969, pp. 903–907.

[20] Phillips, W. M., Keel, A. G., Jr., and Kuhlthau, A. R., "The Measurement of Sphere Drag in a Rarefied Gas Using a Magnetic Wind Tunnel Balance," Rept. AEEP-3435-115-70 VT, April 1970, University of Virginia, Charlottesville, Va.

[21] Kussoy, M. I., Stewart, D. A., and Horstman, C. C., "Sphere Drag in Near-Free-Molecular Hypersonic Flow," *AIAA Journal*, Vol. 8, No. 11, Nov. 1970, pp. 2104–2105.

[22] Kussoy, M. I. and Horstman, C. C., "Cone Drag in Rarefied Hypersonic Flow," *AIAA Journal*, Vol. 8, No. 2, Feb. 1970, pp. 315–320.

[23] Geiger, R. E., "Some Sphere Drag Measurements in Low Density Shock Tunnel Flows," R635D23, July 1963, General Electric, Space Sciences Laboratory, Valley Forge, Pa.

DECEMBER 1973 AIAA JOURNAL VOL. 11, NO. 12

Experimental Study of Supersonic Laminar Base Flow with and without Suction

ANTONI K. JAKUBOWSKI* AND CLARK H. LEWIS†
Virginia Polytechnic Institute and State University, Blacksburg, Va.

Heat-transfer and pressure distributions in laminar separated flows downstream of rearward-facing steps with and without mass suction were investigated at Mach numbers around 4 for the conditions when the boundary-layer thickness was comparable to or larger than the step height. In both suction and no-suction cases, an increase of the step height resulted in a sharp drop of the base heating rates which then gradually recovered to less or near attached-flow values obtained with flat-plate configuration. Mass suction from the step base area increased the local heating rates, this effect was however relatively weak for laminar flows tested and the competing effect of the step height clearly predominated. It was found that even removal of the entire incoming boundary layer was not sufficient to raise the poststep heating rates above the flat-plate values. The base pressure in the no-suction, solid-step case correlated reasonably well with the step height-to-boundary-layer thickness ratio (h/δ) and with the Reynolds number based on the step height ($Re_{\infty,h}$). Our experimental evidence indicated that entrainment conditions at separation may have a significant effect on the pressure distribution and flowfield behind the step. The results and trends observed in this study are discussed and explained qualitatively in terms of the simple flowfield models.

Nomenclature

b = width of model
h = step height
H = enthalpy
L = surface length preceding the step
$\dot{m}$ = mass flow rate
M = Mach number
P = pressure
$\dot{q}$ = heat flux
$Re_{\infty,h}$ = $U_\infty h/\nu_\infty$, Reynolds number based on h
$Re_{\infty,L}$ = $U_\infty L/\nu_\infty$, Reynolds number based on L
T = absolute temperature
U = velocity
w = $\dot{m}_s/\rho_\infty U_\infty bh$, nondimensional mass suction-rate
x = distance downstream of the leading edge
Δx = distance downstream of the step
δ = boundary-layer thickness
δ^* = boundary-layer displacement thickness
ρ = density
ν = kinematic viscosity

Subscripts

b = base
BL = boundary layer
max = maximum value
ns = no suction
o = stagnation conditions
ref = reference value
s = suction; static
step = step location on the flat plate
w = wall or surface value
∞ = freestream conditions

Received December 18, 1972; revision received July 5, 1973. This work was supported by NASA under Grant NGR-47-004-070.

Index categories: Boundary Layers and Convective Heat Transfer—Laminar; Jets, Wakes, and Viscid-Inviscid Flow Interactions; Supersonic and Hypersonic Flow.

* Assistant Professor of Aerospace Engineering.
† Professor of Aerospace Engineering.

Introduction

KNOWLEDGE of the flowfield past a rearward-facing step is important in the aerothermodynamic design of various flight configurations including hypersonic control surfaces and possible application of sliding metallic heat-shield panels for future space shuttle structures. One of the possible flow regimes associated with these configurations, and characteristic of the high altitude phase of re-entry, may involve a thick laminar boundary layer approaching the step (boundary-layer thickness δ comparable to or larger than the step height h) and possibility of mass suction from the base region. It is our intention to investigate heat-transfer and pressure distributions for such flow configurations.

The flowfield in the step region under no-suction conditions is determined by a strong interaction between the viscous recirculating region at the step base and the external inviscid flow. The studies of various aspects of a rearward-facing step or wedge are numerous; however, the vast majority of published works have centered on the case where the boundary-layer thickness is smaller than the step height, including investigations by Rom and Seginer,[1] Weiss and Weinbaum,[2,3] Scherberg and Smith,[4,5] Hama,[6] Batt and Kubota,[7] and more recent works by Erdos and Zakkay,[8] Wu and Su,[9] and Ohrenberger and Baum.[10]

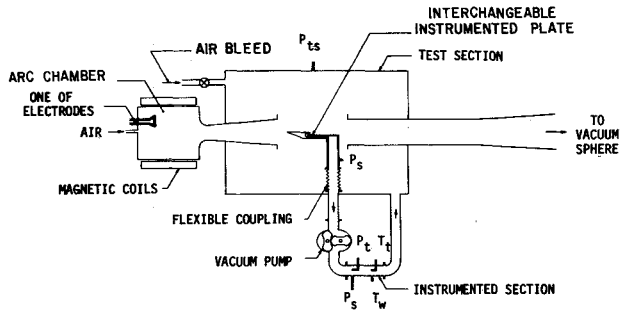

Fig. 1 Schematic diagram of experimental set-up with Model II.

Experimental information on the case of $h/\delta \leqq 1$ is almost nonexistent and, to our knowledge, no experiments have been made that would include mass suction from the separated area.

When the boundary-layer thickness is comparable to or larger than the step height then: a) downstream effects can be easily transmitted upstream through the subsonic portion of the boundary or shear layer, b) viscous effects may increase their range of influence, and c) the effects characteristic of supersonic, thin boundary-layer flow such as expansion at the corner, well-defined location of compression near the reattachment point, and configuration of lip and trailing shocks will be substantially modified. Further modification and/or complexity will be introduced by application of the mass suction from the step base. Such a suction may conceivably result in an intense heating at reattachment and, therefore, knowledge of poststep heat-transfer distribution, when the mass suction is applied, may be of considerable practical importance. In addition, it is felt that a study of pressure and heat-transfer distributions may provide information which can be used to define preliminary flowfield models amenable to analytical studies.

Our experiments were conducted at $M_\infty \approx 4$ in an arc-heated wind tunnel of the Thermal Facility Unit at NASA Langley. The ratio h/δ varied from 0.1 to 2.4 and the ratio of wall temperature to freestream stagnation temperature, T_w/T_o, varied between 0.055 and 0.11. The effects on surface pressure and heating rates of step height, slot mass-flow rate, and freestream flow parameters are presented and discussed for a range of $Re_{\infty,h}$ (Reynolds number based on freestream conditions and step height) between 40 and 2200. The present data on base pressure and maximum poststep heating rates are correlated and compared with available theoretical predictions.

Experimental Apparatus and Procedures

The arc-heated wind tunnel used for the experiments consists of a magnetically-stabilized ac arc heater, plenum chamber, a 15° conical supersonic nozzle, test cabin, and a diffuser which exhausts into a vacuum sphere at minimum pressure of approximately 1 mm Hg. The watercooled supersonic nozzle has a 7-cm-diam throat and a 22.8-cm-diam exit section. The size of uniform gas core at the model location is no less than 17 cm. The test medium was air heated by copper electrodes and the nominal range of test conditions was: $P_o = 1.82 \times 10^4 - 1.99 \times 10^5$ N/m^2 (0.18–1.96 atm), $T_o = 2700$–5500°K, $M_\infty = 3.95$–4.27, Re_∞/cm = 160–2200.

Two copper, water cooled models were used in this investigation. Model I was designed for no-suction tests and had a solid step-face. Model II was designed and used primarily for suction tests. Both models were two dimensional, without side plates, and provided with sharp leading edges and with rearward-facing steps of adjustable height. The maxium step height was 1.02 cm on both models, and the flat-plate sections preceding the step on Models I and II were 12.5 cm and 10 cm long, respectively.

Model II was designed as an integral part of a structure containing the step model itself, retractable supporting strut and air suction duct. Under the conditions of thick approaching boundary layers and low pressures in the base region, a large suction flow area was required in order to remove a significant portion, or possibly, the entire boundary-layer flow. Therefore, nearly the entire area of the vertical step face was used as a suction slot. The slot was connected to an R-6000 Heraeus Mechanical Blower via a system of flexible hoses which allowed for rapid injection of the model into the test stream. The discharge side of the blower was connected to an instrumented pipe section which contained several sensors of pressure (static and total) and temperature to provide information necessary for evaluation of suction-mass flow-rate. A simplified diagram of the experimental setup used in tests on Model II is presented in Fig. 1.

Both models were equipped with interchangeable reattachment plates mounted just downstream of the steps. The reattachment plates used for heat-transfer measurements were made of a 0.74-mm-thick stainless-steel sheet and were instrumented with chromel-alumel thermocouples spot-welded to the undersurface. Heat-transfer data were obtained from measurements of transient skin temperatures resulting from a stepwise increase in stagnation temperature. The model, initially at room temperature, was suddenly exposed to the hot air flow where it remained from 1 sec to 3 sec. Skin temperatures were recorded at a rate of 40 measurements per second. Preliminary experiments indicated that the slope dT_w/dt (wall temperature vs time) remained very nearly constant for at least 3 sec which was much longer than the time period required to stabilize pressures in the suction circuit (less than 0.8 sec). On this basis we assumed that the heat-transfer measurements were not affected by the heat conduction within the reattachment plate.

Reattachment plates designed for pressure measurements were made of copper and were water cooled. Pressure measurements on Model I included measuring two pressures on the upstream section: "reference" pressure at 3.1 cm ahead of the step and the pressure on the vertical surface of the step.

Test Conditions

Freestream Properties

Tunnel flow properties were determined from both measurements and calculations. During each experiment, the pitot pressure and stagnation-point heat-transfer rate were measured at the model location and the plenum pressure was measured in the arc chamber. The stagnation enthalpy was then determined for dissociated air in thermochemical equilibrium using a correlation based on Fay and Riddell's theory. The freestream properties at the step location were determined, taking account of the nozzle nonequilibrium flow. The stagnation conditions (the measured plenum pressure and the corresponding equilibrium temperature obtained from a Mollier diagram using the appropriate stagnation enthalpy) were used as input data for the computer program for frozen-flow isentropic expansions.[11] The solution was terminated at the station where the computed pitot pressure matched the pitot pressure measured at the step location.

The assumption of the frozen flow model was based on an independent study which included numerical calculations[11] of a) nonequilibrium, b) frozen, and c) equilibrium nozzle expansions for a number of test conditions spanning the entire range of the nominal conditions. The results of those calculations showed clearly that, in all cases, the flow properties defined from frozen flow expansions were very close to the properties determined from nonequilibrium flow expansions, and therefore, the use of simple frozen expansions should be considered as a reasonable assumption. An additional argument on behalf of this assumption was provided by close agreement between the measured wall pressure distributions on the flat-plate configuration and the theoretical predictions based on frozen flow properties. In making such predictions, account was made for the existence of a longitudinal pressure gradient in the test section which was identified from pitot pressure surveys.

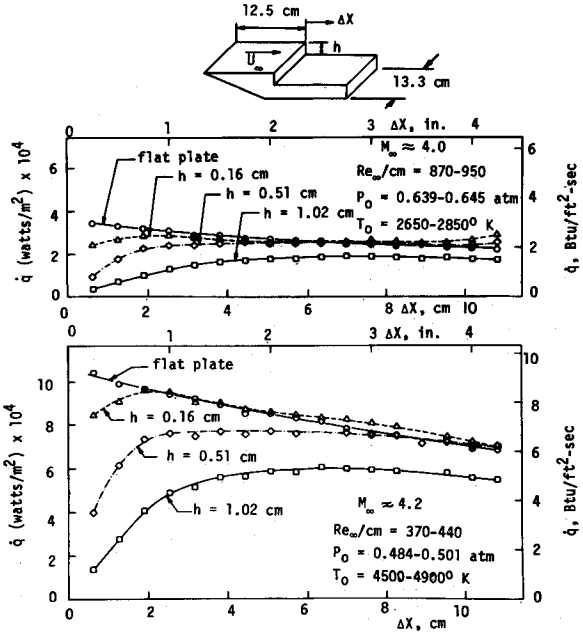

Fig. 2 Heat-transfer distribution downstream of the step: Model I.

Boundary-Layer Parameters

In the case of a thick laminar boundary layer the base pressure may exert a strong influence in the upstream direction and the parameters of the boundary layer at the step location may be significantly modified when compared with a no-step configuration. The upstream influence of the base pressure is discussed in Ref. 12. To characterize the boundary layer approaching the step area we need a reference parameter which excludes the effects of the step itself. The thickness of the boundary layer along the flat plate at the step location, δ, may serve as a convenient reference parameter. Predictions of the boundary-layer parameters along the flat plate were obtained for nonequilibrium flow-equilibrium catalytic wall conditions.[13] The selection of these particular conditions was based on critical evaluation of numerical predictions of flat-plate heat-transfer distributions obtained for the models as follows: a) nonequilibrium flow-equilibrium catalytic wall, b) nonequilibrium flow-noncatalytic wall, and c) perfect gas flow. It was found that in practically all cases being compared (sixteen different test conditions), the predictions based on the model a) were in close agreement with the experimental data, whereas the predictions using the other two models underestimated heating rates by a large margin.

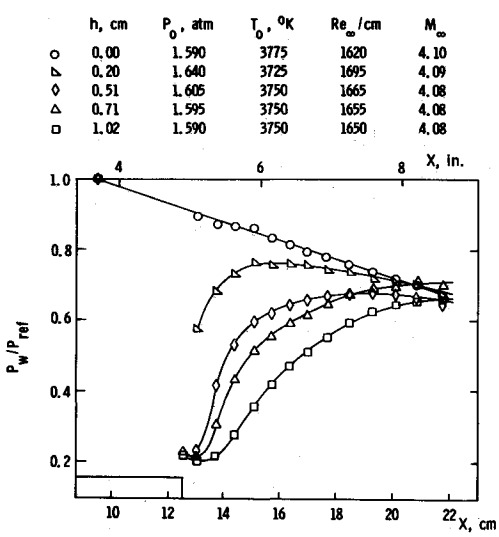

Fig. 3 Surface pressure distribution downstream of the step: Model I.

Flow Uniformity

As we mentioned previously, pitot pressure surveys revealed the presence of a longitudinal pressure gradient in the test section. The presence of the pressure gradient was accounted for in numerical calculations of the boundary layer along the flat-plate models as well as pressure and heat-transfer distributions.

Transverse surveys of pressure distribution on the reattachment plate demonstrated that the flow along the instrumented part of the plate was two-dimensional over a distance of at least 6.5 cm downstream of the step, and for most of the test conditions, it remained two-dimensional along 9 cm behind the step. The rear portion of the plate was, at some conditions, influenced by back pressure effects or a shock system generated by the supporting strut; however, that part of the flow extended well beyond the separated flow region which was the main object of this investigation.

Results and Discussion

No-Suction Case (Model I)

Figure 2 presents typical poststep heat-transfer distributions obtained with three different step heights and compared with heat-transfer distribution of a flat-plate configuration. For the largest step ($h = 1.02$ cm), the heating rates at the step base are significantly lower than the attached-flow values (obtained with flat-plate configuration) and they recover more or less gradually to somewhat less than the attached-flow values near the approximate reattachment region. For the smaller steps, the heating rates downstream of the reattachment region are approximately equal to the attached-flow values. With a large step, the heating rate at the step base was found to be nearly insensitive to the stagnation pressure change by a factor as large as eight and was only slightly affected by the changes in the stagnation temperature. Thus, the step height appears to play the dominant role in establishing heat-transfer rate at the step base. Moving further downstream, the step influence is gradually phased out and the heating rates become determined mostly by the freestream properties of the main flow. The maximum heating rate occurred at a distance which varied from about 6 step heights for the largest step (1.02 cm) to about 14 step heights for the smallest step (0.16 cm).

Typical distributions of surface pressure behind the steps of different height are displayed in Fig. 3. The pressures are normalized by the value of the reference pressure, P_{ref}, measured upstream of the step ($\Delta x = -3.1$ cm). Pressure distributions indicate a small region of low pressure immediately downstream of the step. The length of this region tended to increase with the step height h and freestream Reynolds number Re_∞. Downstream of this low pressure "plateau," the pressure increased rapidly and, at distances of a few step heights, it recovered to approximately the attached-flow values of the flat plate. Since

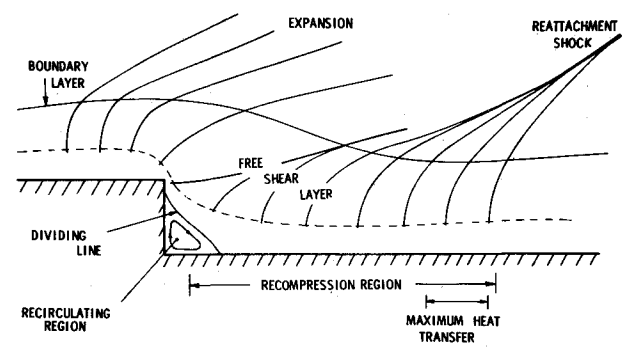

Fig. 4 Hypothetical scheme of flowfield in experiments on Model I. Laminar boundary layer, $h/\delta \sim 0(1)$.

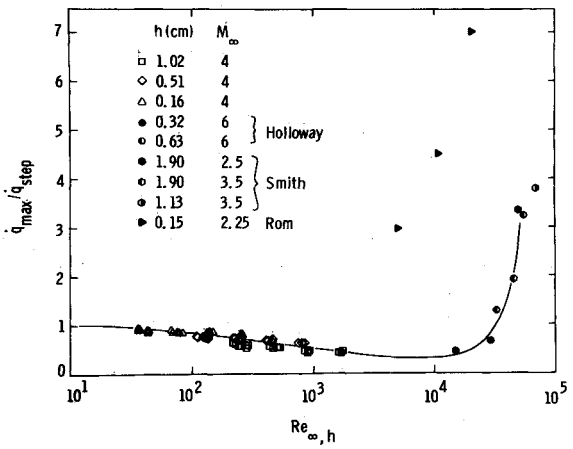

Fig. 5 Maximum heating rate as function of $Re_{\infty,h}$.

the low-pressure region at the step base is, most likely, associated with a recirculating flow, we may infer that for the conditions of laminar flow and thick incoming boundary layers, the extension of the recirculating area is very small, being less than one step height in most of these experiments.

The trends observed in experiments on Model I may be explained qualitatively by referring to a hypothetical schematic of the flowfield model believed to be characteristic for the case of a thick laminar boundary layer (boundary-layer thickness, δ, comparable with the step height, h) (Fig. 4). An increase of the step height results in a) an increased expansion around the step corner leading to a rather sharp drop in the base pressure and hence a lower density at the step base and b) an increased thickness of the recirculating region which causes a reduction of temperature gradients near the wall. Both these effects are responsible for a significant drop in heating rates behind the step, when its height is increased. In addition, at a higher step, the shear layer is subject to mixing with relatively cool recirculating air over a longer period and length which leads to a "cooling" and some additional lateral expansion of the shear layer, and as a consequence, the temperature gradients and levels near the wall in the recompression zone are reduced and so are the heating rates. In consistency with the presence of a very small recirculating region in these tests, heating rates (and pressures) started to recover from low base values almost immediately downstream of the step. The maximum heating rate is expected to occur in the neighborhood of the maximum convergence (neck) of the reattaching shear layer, where both the temperature gradient and mass flux are likely to attain their maximum values. Thus, according to this suggestion, the maximum heat transfer may occur far downstream of the stagnation point (i.e., the point where the dividing streamline meets the surface of the plate) and this is in some variance with the commonly accepted model for heat-transfer distribution in separated flows.

Figures 5–7 present the correlations of the peak heating rates against the parameters $Re_{\infty,h}$ and h/δ. The peak heating rates,

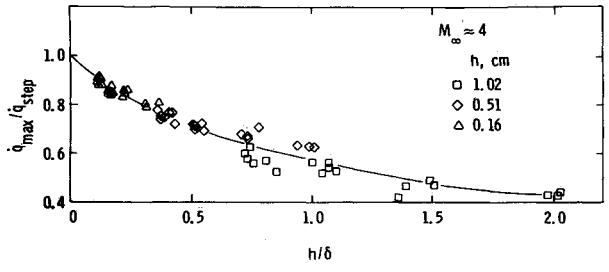

Fig. 6 Maximum heating rate as function of h/δ.

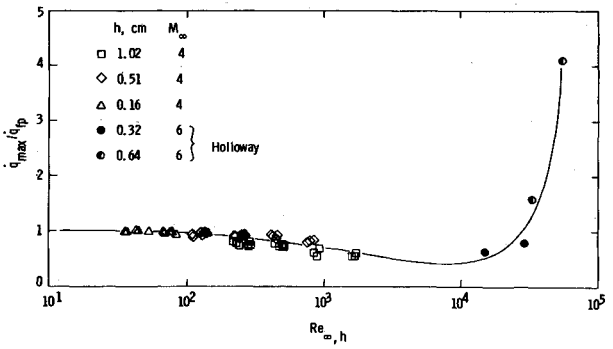

Fig. 7 Maximum heating rate as function of $Re_{\infty,h}$.

$\dot{q}_{max}$, are referenced to heating rates at the step location obtained from flat-plate measurements, $\dot{q}_{step}$, (Figs. 5 and 6) or to local flat-plate values, $\dot{q}_{fp}$ (Fig. 7). At a given Mach number, the parameter $Re_{\infty,h}$ combines the effects of the freestream Reynolds number Re_∞ and the step height, h. For a given model geometry (L/h) and a laminar boundary layer, the parameter $Re_{\infty,h}$ varies as $(h/\delta)^2$. This emphasizes the potential effectiveness of $Re_{\infty,h}$ as a scaling factor because the step height and the boundary-layer thickness are the length scales which control the flowfield in the separated region. Figures 5 and 7 include data obtained by Rom and Seginer,[1] Smith,[5] and several points evaluated on the basis of measurements reported by Holloway, Sterrett, and Creekmore.[14] The combination of our results with the results of Smith and those of Holloway et al. provides a continuous variation of peak heating-rates over the range $10^2 < Re_{\infty,h} < 10^5$. The results of Rom and Seginer depart very strongly from other reported results. It should be pointed out that Rom's measurements were made in a shock tube using very small models. A line traced through the experimental points represents "average" $\dot{q}_{max}/\dot{q}_{step}$ or $\dot{q}_{max}/\dot{q}_{fp}$ values at supersonic speeds ($M < \sim 6$). According to this line, a flat minimum may occur somewhere around $Re_{\infty,h} \approx 10^4$. The magnitude of this minimum may depend on the freestream Mach number M_∞, however, we do not expect any strong effect of M_∞ in the range $Re_{\infty,h} < 10^3$. A physical explanation of the peak heating-rate variation shown in Fig. 5 can be given in terms of the combined effects of Re_∞ and h as follows:

1) In the range of low Re_∞ covered by our experiments ($Re_{\infty,h} < 2 \times 10^3$) and for a given geometry (L, h), an increase of the unit Reynolds number is equivalent to a reduction of the boundary-layer thickness δ, which in turn results in an extension of the recirculating region and moving the location of the peak heat transfer $\dot{q}_{max}$ further downstream. Consequently, the ratio $\dot{q}_{max}/\dot{q}_{step}$ reduces somewhat when Re_∞ increases (note that $\dot{q}_{max}$ values were near or less than flat-plate heating rates and the latter decreased in the downstream direction). The effect of the step height in the low Re_∞-range, discussed previously, can be briefly summarized as follows: The larger h is, the lower the base heating will be, the further downstream the heat-transfer reducing influence of h extends, and consequently $\dot{q}_{max}$ occurs further downstream resulting in lower values of $\dot{q}_{max}/\dot{q}_{step}$. Hence, both Re_∞ and h, when being increased, affect $\dot{q}_{max}/\dot{q}_{step}$ in the same direction, and, as the parameter $Re_{\infty,h}$ increases from very small values, the ratio $\dot{q}_{max}/\dot{q}_{step}$ gradually decreases from the initial value of unity.

2) As the Reynolds number and/or step height increase ($Re_{\infty,h} > \sim 10^3$) the effects of Re_∞ and h tend first to stabilize and then become reversed. For this we offer an explanation as follows: When the boundary-layer thickness becomes several times smaller than the step height (due to increasing Re_∞ at a given h), then the upstream penetration of base pressure will be reduced, the recirculating region will expand, and the regions of expansions and recompressions become relatively contracted streamwise and separated by a free shear layer of nearly constant pressure. Because the recompression region becomes

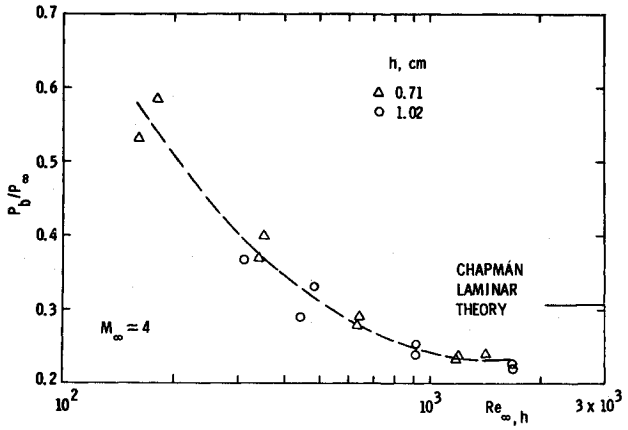

Fig. 8 Base pressure as function of $Re_{\infty,h}$.

more confined streamwise and its thickness relative to the step height decreases, the heating rates must increase above the flat-plate values if the boundary layer continues to decrease in thickness. This of course will be followed by an increase of $\dot{q}_{max}/\dot{q}_{step}$ values. As for the effect of the step height itself, it has been shown in our experiments (cf. Fig. 8) that above $Re_{\infty,h} \approx 10^3$, the base pressure tends to stabilize and becomes rather insensitive to the step height (in a purely laminar flow). This should be followed by a somewhat similar behavior of heating rates. At sufficiently large Reynolds number, we may expect an onset of transition effects in the separated area, and this will bring about some new and possibly drastic changes in the variation of $\dot{q}_{max}/\dot{q}_{step}$.

The correlations of base pressure data are shown in Figs. 8 and 9, where the base pressure ratios, P_b/P_∞, are plotted against parameters $Re_{\infty,h}$ and h/δ. The values of P_∞ correspond to the step location and were taken from the experimental pressure distributions along the flat-plate configuration.‡ The variation of P_b/P_∞ displays an initial decrease with a tendency toward leveling-off in the upper ranges of $Re_{\infty,h}$ and h/δ tested. The plot of P_b/P_∞ against h/δ demonstrates clearly that, for laminar separated flows, h and δ are the length scales which control the base pressure. Figure 9 includes some theoretical results recently published by Inger (Ref. 15). His predictions on the initial slope of the base pressure variation with h/δ (for $h/\delta < 1$) agree well

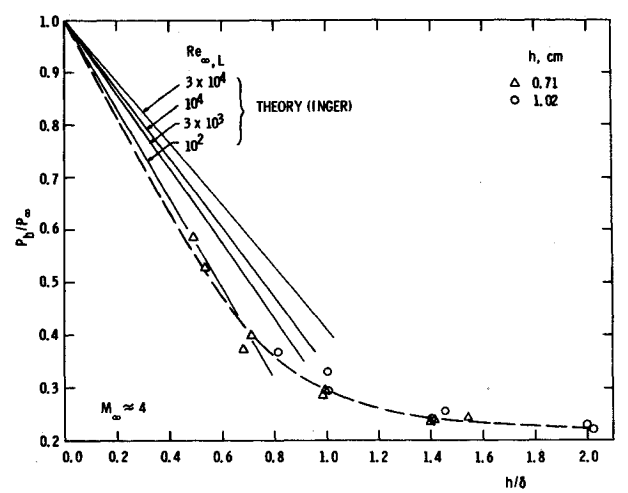

Fig. 9 Base pressure as function of h/δ.

‡ Because of some uncertainty involved in measurements of P_b at small step height ($h \leq 0.51$ cm), we did not include the data for $h \leq 0.51$ cm. It should be mentioned, however, that the data for small steps followed the same trends as shown in Figs. 7 and 8.

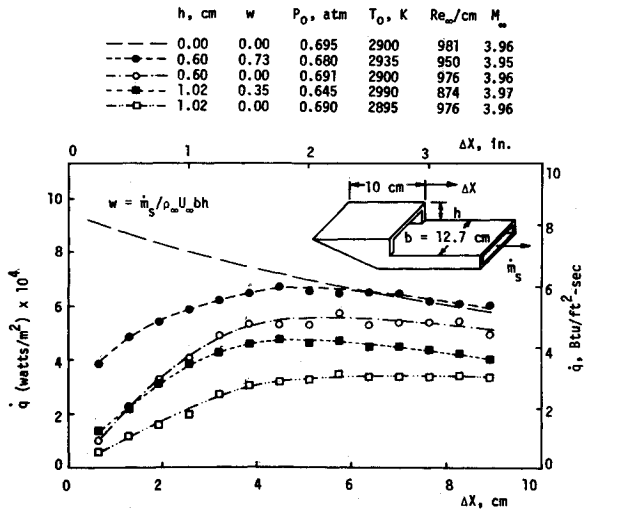

Fig. 10 Effect of mass suction on poststep heat-transfer distribution: Model II.

with our results (note that our data in the range $h/\delta < 1$ correspond to $Re_{\infty,L} < 3 \times 10^3$). Our results seem to indicate that the conclusion of Chapman et al.[16] and Denison and Baum[17] that the base pressure is independent of Re_∞ for laminar flow may be essentially correct at $Re_{\infty,L} > 10^4$, even in the case of thick boundary layers.§ The base pressure predicted by the laminar theory of Chapman[17] is shown in Fig. 8. It may be pointed out that several investigators who studied laminar near wakes behind slender wedges and cones[19-21] reported the same trend in the base pressure variation as the one observed in our experiments. At the same time, conclusions of Kavanau[22] and Weiss[23] who predicted an increase of P_b/P_∞ until $Re_{\infty,L} \approx 10^4$, are at variance with our results.

Suction Case (Model II)

Typical heat-transfer distributions downstream of 1.02 cm and 0.6 cm step heights, obtained for "suction" and "no-suction" cases and compared with "reference" distribution of a flat-plate configuration under similar freestream conditions, are shown in Fig. 10. The no-suction measurements were made with the suction duct blanked off at the model outlet-port, thus leaving a large internal cavity connected to the suction slot. The nondimensional mass-suction rate, w, is defined as the ratio of the mass flow rate through the slot, $\dot{m}_s$, to a mass flow rate based on freestream conditions and the step surface, $\rho_\infty U_\infty bh$.

Our experiments showed that, in general, mass suction from the separated area increased the local heating rates. The relative increase depended on a) freestream conditions of the main flow, b) rate of mass suction, c) step height, and d) location behind the step. The maximum heating rate occurred at distances of 4–6 step heights behind the 1.02-cm step and 7–9 step heights behind the 0.6-cm step. In terms of the maximum heating rate, even large suction rates, applied in this investigation, did not produce any spectacular peaks and the effect of mass suction seemed to be weaker than might be expected. Nevertheless, at sufficiently large values of w, local heating rates due to mass suction approached or exceeded the corresponding values of the flat-plate configuration. It appears that the suction case is governed primarily by two parameters, h and $\dot{m}_s$. The heating rates decrease with increasing h, but increase with increasing $\dot{m}_s$. Of these two competing effects, the former clearly predominates for the flow configuration and freestream Reynolds number range studied.

No-suction heat-transfer distributions obtained on slotted-step

§ Chapman's model assumes a zero initial boundary-layer thickness, whereas Denison and Baum's model assumes a finite but relatively small boundary-layer thickness.

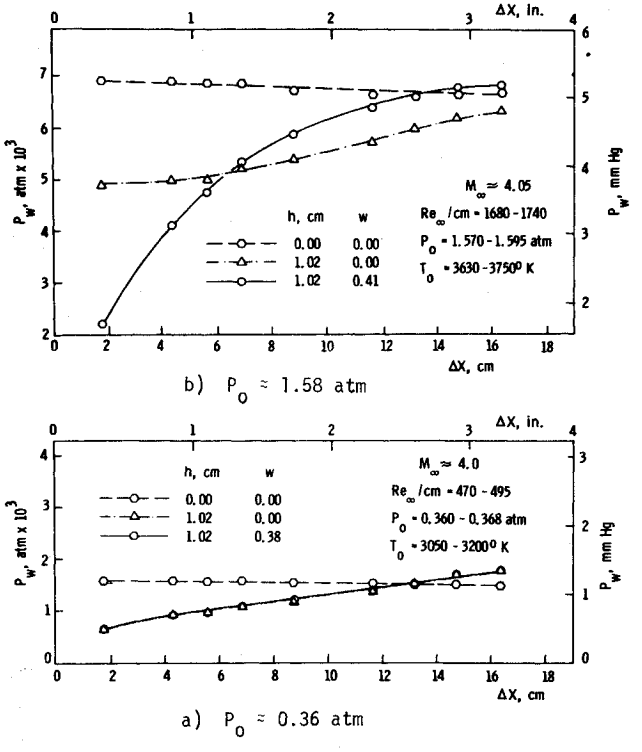

Fig. 11 Effect of mass suction on poststep pressure distribution: Model II.

model (Model II) differed somewhat from those obtained on solid-step model (Model I), the main difference being a slower recovery of heating rates downstream of the base and, correspondingly, slightly lower peak values in the slotted-step case. Only part of the difference can be ascribed to different lengths preceding steps in Models I and II. The main origin of the observed difference seems to be associated with different entrainment conditions at separation (cf. Figs. 4 and 12b). This inference can be reached on examination of pressure distributions downstream of the slotted step (measured with and without mass suction, Fig. 11) and comparing them with solid-step pressure distributions. At low stagnation pressures (Fig. 11a), no-suction data coincided practically with the suction data. As the pressure level increased (Fig. 11b), the no-suction pressure distributions departed from the suction case, exhibiting a relatively small pressure drop around the step, followed by a slow and gradual pressure increase behind the step base.

The trends observed in heat-transfer and pressure distributions can be explained in terms of hypothetical flowfield models as sketched in Fig. 12. When the mass suction is applied (Fig. 12a), the flow downstream of the step base is formed by a boundary layer which develops along the surface while remaining under a strong influence of the recompression occurring in the adjacent outer flow. In essence, pressure and heat-transfer distribution in the suction case are similar to those observed in the no-suction solid-step case (Model I), the main difference being a somewhat

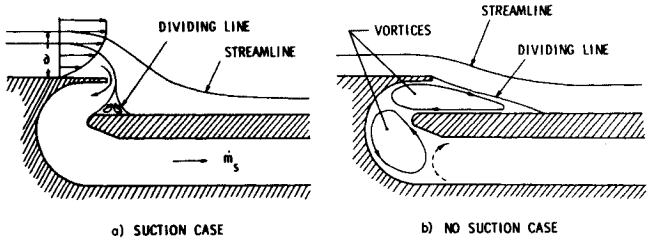

Fig. 12 Flowfields in tests on Model II.

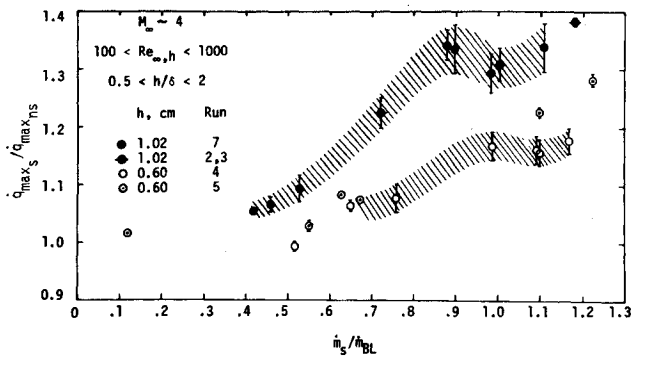

Fig. 13 Increase in maximum heating rate as function of boundary-layer removal.

smaller streamwise extension of the recompression zone in the suction case. In the case of no-suction open-slot step, a system of vortices may develop as sketched in Fig. 12b. The pressure at the step base, and correspondingly, the amount of expansion in the flow over the step, may be strongly affected by a relatively extended viscous-flow region beneath the step and shear layer and by the amount of pressure differential which can be maintained across this region. Since no large pressure difference can be sustained by a low-energy flow, hence at stream pressures higher than a certain value, the "base-pressure" departs strongly from the value corresponding to a solid-step configuration and remains only somewhat lower than the freestream static pressure. In contrast, in the no-suction solid-step case (cf. Fig. 4), the viscous dominated region is very limited and the base pressure seems to be governed primarily by the properties of the outer inviscid flow (and the geometry of the step), even at low Reynolds numbers characteristic of these experiments.

From the viewpoint of potential practical applications of step geometry involving suction, the most important property may be the maximum poststep heating rate. Figure 13 illustrates how the maximum heating rate recorded with suction applied $\dot{q}_{max_s}$ and normalized by the maximum heating rate without suction $\dot{q}_{max_{ns}}$ (using the same configuration, i.e., slotted-step model), varies with the ratio of mass-suction rate, $\dot{m}_s$, to the boundary-layer mass flow rate, $\dot{m}_{BL}$. The latter was calculated from

$$\dot{m}_{BL} = \int_o^\delta \rho u \, dy$$

for a number of test conditions. Since the stagnation conditions in the tests being compared usually differed somewhat, corrections had to be applied to the values of $\dot{q}_{max_s}/\dot{q}_{max_{ns}}$ which involved some uncertainty. Consequently, most of the experi-

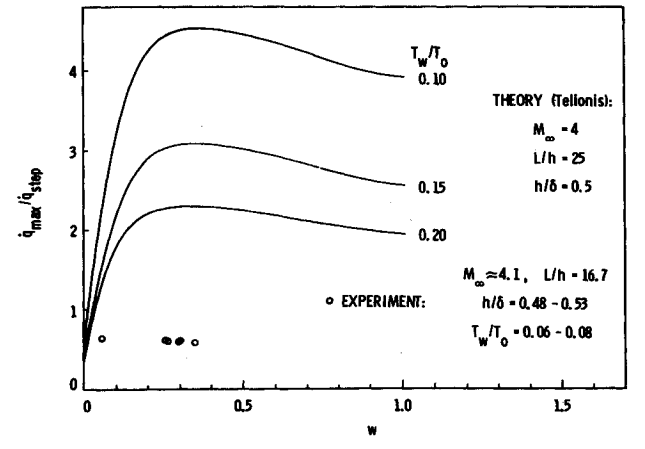

Fig. 14 Increase in maximum heating rate as function of w.

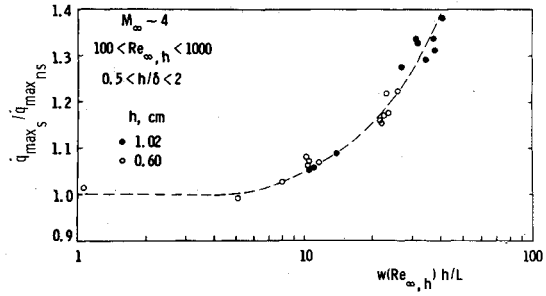

Fig. 15 Correlation of maximum heating-rate increase due to mass suction.

mental points are indicated in the form of bars which span from the minimum to the maximum of expected values. The most complete, and, perhaps most reliable data were collected in runs 4 and 7 with the steps of 0.6 and 1.02 cm, respectively. These results, displayed in Fig. 13 as shaded areas, indicate that as the mass removal increases and approaches $\dot{m}_{BL}$, the ratio $\dot{q}_{max_s}/\dot{q}_{max_{ns}}$ tends to level off. Such a behavior should be expected on the grounds of temperature distribution across the boundary layer. A subsequent small reduction in $\dot{q}_{max_s}/\dot{q}_{max_{ns}}$, which can be seen in the results of runs 4 and 7, may or may not be fortuitous and we see no simple explanation of such a variation. In Fig. 14, we plotted the ratio $\dot{q}_{max_s}/\dot{q}_{step}$ against the nondimensional mass-suction rate w for the case of $h/\delta \approx 0.5$. For this particular case of h/δ, theoretical predictions have been recently published in Ref. 24. A very strong departure of these predictions from the experimental results is evident, particularly if one notes that theoretical plots corresponding to T_w/T_o values in our experiments (0.06–0.08) would lie well above those depicted in Fig. 14. Figure 15 attempts to correlate all suction data by using the parameter $w(h/L)\,Re_{\infty,h}$ as the scaling factor. At very small values of this parameter, including the case of no suction [i.e., $w(h/L)\,Re_{\infty,h} = 0$], the ratio $\dot{q}_{max_s}/\dot{q}_{max_{ns}}$ is close to unity. As the parameter increases above about 5 the heating-rate amplitude $(\dot{q}_{max_s}/\dot{q}_{max_{ns}})$ starts to increase. We may note that the parameter $w(h/L)\,Re_{\infty,h}$ is roughly proportional to suction-mass flow rate and it increases rapidly with the step height $[w(h/L)\,Re_{\infty,h} \sim h^2]$, thus pointing to the fact that the step height plays a dominant role in establishing heating rates at the step base.

Conclusions

An experimental study was conducted to determine heat-transfer and pressure distributions in laminar supersonic flows downstream of rearward-facing steps without and with mass suction from the separated region. Flow and test conditions varied in the ranges as follows: $M_\infty \approx 4$, $40 < Re_{\infty,h} < 2200$, $0.1 < h/\delta < 2.4$, $0.055 < T_w/T_o < 0.11$, and $0.1 < w < 0.8$. The more important results of this study are presented below.

1) For both suction and no-suction cases, an increase in the step height caused a sharp drop in the initial heating rates (at the step base) which then gradually recovered to less or near the attached-flow values. The height of the step controlled the heating rates at the step base, clearly dominating effects of stagnation temperature and pressure.

2) In the Re_∞-range studied, the ratio of the maximum heat-transfer in the recompression zone to the attached-flow value at the step $(\dot{q}_{max}/\dot{q}_{step})$ was less than unity and decreased slowly with h/δ or $Re_{\infty,h}$. It is anticipated that in the no-suction case, $\dot{q}_{max}/\dot{q}_{step}$ attains a minimum somewhere around $Re_{\infty,h} \sim 10^4$. The variation of the maximum heat transfer referenced to the local attached-flow value $(\dot{q}_{max}/\dot{q}_{fp})$ was very similar to the variation of $\dot{q}_{max}/\dot{q}_{step}$.

3) Mass suction from the separated area increased the local heating rates, the relative increase being most significant immediately behind the step. In general, however, the effect of mass suction on heat transfer at all-laminar flows was relatively weak and a mass suction rate exceeding the mass flow rate of the entire incoming boundary layer was needed to raise the post-step heating rates above the flat-plate values. Mass-suction data expressed in terms of the ratio $\dot{q}_{max_s}/\dot{q}_{max_{ns}}$ (peak heating rate with suction ratioed to the peak heating rate without suction) was correlated by using a parameter $w(h/L)\,Re_{\infty,h}$.

4) Pressure distribution downstream of the step was found to be dependent on the entrainment conditions at separation. In the no-suction solid-step case, the base pressure correlated reasonably well with the parameters $Re_{\infty,h}$ and h/δ, displaying an initial decrease followed by a tendency to level-off in the upper range of $Re_{\infty,h}$ and h/δ tested. The length of a pressure plateau behind the step was very small and tended to increase somewhat with Re_∞ and h. In the mass-suction case, the post-step pressure distributions resembled generally those obtained on no-suction solid-step configuration.

References

[1] Rom, J. and Seginer, A., "Laminar Heat Transfer to a Two-Dimensional Backward Facing Step from the High-Enthalpy Supersonic Flow in the Shock Tube," *AIAA Journal*, Vol. 2, No. 2, Feb. 1964, pp. 251–255.

[2] Weiss, R. and Weinbaum, S., "Hypersonic Boundary Layer Separation and the Base Flow Problem," *AIAA Journal*, Vol. 4, No. 8, Aug. 1966, pp. 1321–1330.

[3] Weiss, R. F., "A New Theoretical Solution of the Laminar, Hypersonic Near Wake," *AIAA Journal*, Vol. 5, No. 12, Dec. 1967, pp. 2142–2149.

[4] Scherberg, M. G. and Smith, H. E., "An Experimental Study of Supersonic Flow over a Rearward Facing Step," *AIAA Journal*, Vol. 5, No. 1, Jan. 1967, pp. 51–56.

[5] Smith, H. E., "The Flow Field and Heat Transfer Downstream of a Rearward Facing Step in Supersonic Flow," ARL 67-0056, March 1967, Aerospace Research Lab., Wright-Patterson Air Force Base, Ohio.

[6] Hama, F. R., "Experimental Studies on the Lip Shock," *AIAA Journal*, Vol. 6, No. 2, Feb. 1968, pp. 212–219.

[7] Batt, R. G. and Kubota, T., "Experimental Investigation of Laminar Near Wakes Behind 20° Wedges at $M = 6$," *AIAA Journal*, Vol. 6, No. 11, Nov. 1968, pp. 2077–2083.

[8] Erdos, J. I. and Zakkay, V., "Inviscid Solution of the Steady, Hypersonic Near Wake by a Time-Dependent Method," *AIAA Journal*, Vol. 9, No. 7, July 1971, pp. 1287–1293.

[9] Wu, J. M. and Su, M. W., "Measurements on Separated Supersonic Boundary Layer Flows After an Expansion Corner," *Proceedings of the Ninth International Symposium on Space Technology and Science*, Tokyo, Japan, 1971.

[10] Ohrenberger, J. T. and Baum, E., "A Theoretical Model of the Near Wake of a Slender Body in Supersonic Flow," *AIAA Journal*, Vol. 10, No. 9, Sept. 1972, pp. 1165–1172.

[11] Lordi, J. A., Mates, R. E., and Moselle, J. R., "Computer Program for the Numerical Solution of Nonequilibrium Expansions of Reacting Gas Mixtures," Rept. AD-1689-A-6, Oct. 1965, Cornell Aeronautical Lab., Buffalo, N.Y.

[12] Wu, J. M., Su, M. W., and Moulden, T. H., "On the Near Flow Field Generated by the Supersonic Flow Over Rearward Facing Steps," Rept. 71-0243, Nov. 1971, Aerospace Research Labs., Wright-Patterson Air Force Base, Ohio.

[13] Blottner, F. G., "Nonequilibrium Laminar Boundary Layer Flow of Ionizing Air," Rept. R64SD56, Nov. 1964, General Electric, Philadelphia, Pa.

[14] Holloway, P. F., Sterrett, J. R., and Creekmore, H. S., "An Investigation of Heat Transfer within Regions of Separated Flows at a Mach Number of 6.0," TN D-3074, Nov. 1965, NASA.

[15] Inger, G. R., "Supersonic Laminar Boundary Layer Flow Past a Small Rearward-Facing Step Including Suction," VPI-E-72-17, 1972, Virginia Polytechnic Inst. and State Univ., Blacksburg, Va.

[16] Chapman, D. R., Kuehn, D. M., and Larson, H. K., "Investigation of Separated Flows in Supersonic and Subsonic Streams with Emphasis on the Effect of Transition," Rept. 1356, 1958, NASA.

[17] Denison, M. R. and Baum, E., "Compressible Free Shear Layer with Finite Initial Thickness," *AIAA Journal*, Vol. 1, No. 1, Jan. 1963, pp. 342–349.

[18] Chapman, D. R., "An Analysis of Base Pressure at Supersonic Velocities and Comparison with Experiments," TR 1051, 1951, NACA.

[19] Dewey, C. F., Jr., "The Near Wake of a Blunt Body at

Hypersonic Speeds," *AIAA Journal*, Vol. 3, No. 6, June 1965, pp. 1001–1010.

[20] Softley, E. J. and Graber, B. C., "An Experimental Study of the Pressure and Heat Transfer on the Base of Cones in Hypersonic Flow," *AGARD Conference Proceedings*, No. 19, Vol. 1, May 1967.

[21] Bauer, A. B., "Some Experiments in the Near Wake of Cones," *AIAA Journal*, Vol. 5, No. 7, July 1967, pp. 1356–1358.

[22] Kavanau, L. L., "Base Pressure Studies in Rarefied Supersonic Flows," *Journal of the Aeronautical Sciences*, Vol. 23, No. 3, March 1956, pp. 193–208.

[23] Weiss, R. F., "Base Pressure of Slender Bodies in Laminar, Hypersonic Flow," *AIAA Journal*, Vol. 4, No. 9, Sept. 1966, pp. 1557–1559.

[24] Telionis, D. P., "Heat Transfer at Reattachment of a Compressible Flow over a Backward Facing Step with a Suction Slot," *AIAA Journal*, Vol. 10, No. 8, Aug. 1972, pp. 1108–1110.

DECEMBER 1973 AIAA JOURNAL VOL. 11, NO. 12

Numerical Analysis of Eddy Viscosity Models in Supersonic Turbulent Boundary Layers

J. S. SHANG,* W. L. HANKEY JR.,† AND D. L. DWOYER‡
Aerospace Research Laboratories, Wright-Patterson Air Force Base, Ohio

Three multilayer eddy viscosity models by Herring-Mellor, Cebeci-Smith-Mosinskis, and Maise-McDonald are compared in this investigation. The aforementioned models were incorporated into an implicit finite difference numerical scheme for compressible turbulent boundary layers. Calculations were performed over Mach number ranges of approximately 0 to 4.55 with the Reynolds number spanning the range of 4×10^6 to 1.41×10^9 for zero pressure gradient and adiabatic wall. All selected viscosity models produced comparable results and provided excellent agreement with the experimental measurements. The calculated results revealed the dominant nature of the viscous sublayer while modifications in the law of the wake region exhibited a relatively mild influence on the numerical solutions.

Nomenclature

C_f = skin-friction coefficient
C_p = specific heat at constant pressure
C = viscosity-density parameter
F = dimensionless velocity u/u_e
h = static enthalpy
k_1, k_2 = constants in eddy viscosity models
L = characteristic length
M = Mach number
P = pressure
Pr = Prandtl number $\mu C_p/\lambda$
T = static temperature
u, v = streamwise and normal velocity components
α = $u_e^2/C_p T_e$
β = $2\xi/u_e(du_e/d\xi)$
γ = ratio of specific heats
δ, δ^* = boundary-layer and displacement thickness
ε = kinematic eddy viscosity coefficient
$\bar{\varepsilon}$ = dimensionless equivalent viscosity $1+\varepsilon/\nu$
$\hat{\varepsilon}$ = dimensionless equivalent viscosity $1+(Pr/Pr_t)(\varepsilon/\nu)$
Θ = dimensionless temperature T/T_e
θ = boundary-layer momentum thickness
λ = molecular thermal conductivity
μ = molecular viscosity coefficient
ν = molecular kinematic viscosity
ξ, η = transformed streamwise and normal coordinates
ρ = density
τ = shear stress

Subscripts
e = denoted variable evaluated at local external stream
t = turbulent property
t,i = beginning of transition
t,f = end of transition
w = denoted variable evaluated at wall
$\langle\ \rangle$ = time-mean average

Presented as Paper 73-164 at the AIAA 11th Aerospace Sciences Meeting, Washington, D.C., January 10–12, 1973; submitted February 12, 1973; revision received July 5, 1973.

Index category: Boundary-Layer and Convective Heat Transfer—Turbulent.

* Aerospace Engineer, Hypersonic Research Laboratory. Member AIAA.

† Senior Scientist, Hypersonic Research Laboratory. Member AIAA.

‡ Captain, U.S. Air Force, Hypersonic Research Laboratory; presently Research Engineer, United Aircraft Research Laboratories, East Hartford, Conn. Student Member AIAA.

Introduction

THE primary purposes of this investigation was to evaluate the classic eddy viscosity model in the regions of the viscous sublayer, the law of the wall, and the law of the wake. Several multilayer eddy viscosity models were chosen for the present purpose. The choice of the classic flux-gradient concept over the turbulent kinetic energy method was based on the fact that for zero pressure gradient situations both methods yielded virtually identical results.[1] One recognizes that both methods could not escape the reign of phenomenological study of turbulent boundary layers. The common weakness manifested itself obviously in the prediction of flows which deviated from the "equilibrium" condition. For the aforementioned reason the present evaluation was restricted to the flows over an adiabatic flat plate.

The viscous sublayer models adopted in the present analysis included the works of Van Driest,[2] Mellor,[3] and McDonald.[4] Van Driest's work on the viscous layer yielded continuous velocity and shear distributions for turbulent flow near a smooth wall. Mellor studied the viscous layer in the light of the similarity law. Noting the different characteristic behavior in